

Many-body calculation of photoionization cross sections in CO

L. Veseth

Department of Physics, University of Oslo, 0316 Oslo, Norway

(Received 16 February 1993)

Total and partial photoionization cross sections are computed for CO at the fixed equilibrium internuclear separation. Finite basis sets were used, with no explicit recourse to continuum orbitals, and there is no need for input of empirical data such as the ionization threshold. By the present method the first step is to compute the (real) polarizability $\alpha(i\eta)$ on the imaginary frequency axis. Many-body perturbation theory is used for that purpose, and the expansion is complete to second order in the Coulomb interaction. In the next step the cross sections are obtained from $\alpha(i\eta)$ by inverting a simple integral equation of the Fredholm first kind (dispersion relation). For the partial cross sections, extra approximations may be necessary, as some diagrams to first and second order make contributions to more than one specific partial cross section. The computed total cross section is in very good agreement with experiment, and good agreement is also obtained for the 1π partial cross section. For the strongly interacting σ shells, the comparison with experiment is less certain. The present results, which include comprehensive correlation corrections, are also compared with existing theoretical results that are on the independent-particle level of accuracy.

PACS number(s): 32.80.Fb, 33.80.Eh

I. INTRODUCTION

The many-body effects encountered in the photoionization of atomic and molecular systems represent a permanent challenge to theorists in the field of atomic and molecular physics. In the atomic case several sophisticated methods have been derived that at least to some extent include correlation effects [1–3]. A common feature of the atomic techniques is that they are based on numerical methods, and explicit wave functions for the outgoing electron have to be found. Thus, the atomic methods are not easily applied to multicenter systems such as molecules.

In the molecular case rather different techniques have been derived based on the use of finite basis sets. The most successful and widely used method so far tends to be the Stieltjes method [4–6], which represents an algebraic approach to the problem without explicit recourse to continuum orbitals. Several molecular calculations have been carried out according to the Stieltjes method [6–11]. Another approach using basis sets is the analytic continuation method [12–15]. Successful applications of the analytic continuation method are, however, so far mostly limited to very small atomic and molecular systems.

Molecular single-center expansions represent a method of carrying atomic techniques over to the molecular systems [16–21]. Various variational techniques may then be combined with the single-center expansion to obtain continuum orbitals in the molecular case [18–23].

Although the molecular methods referred to above should be capable of including many-body effects, little work has been presented that actually includes true correlation effects. Even the most sophisticated methods in current use in the molecular case are on the independent-particle level of accuracy, as only single ex-

citations are included. An example is the random-phase approximation, which is basically similar to the time-dependent Hartree-Fock method. To incorporate what is customarily termed true correlations [24], at least double excitations have to be considered. Even in the atomic case it is well known that independent-particle methods may yield unreliable predictions of the cross sections [2,3], in particular when Hartree-Fock one-electron orbitals are used. The incompleteness of such models is often clearly revealed through large discrepancies between the results obtained with the length and velocity versions of the theory.

It is certainly of considerable interest to find simple and workable independent-particle methods that yield reasonable agreement with experiment, as such models are basic to our physical understanding of the ionization process. However, even in cases like the present example where such simple models are quite successful, it is nonetheless of great importance to investigate the many-body effects with the objective of a more comprehensive and profound theoretical description.

The present work presents computations of the total and partial photoionization cross sections for CO based on many-body perturbation expansions to second order in the Coulomb interaction. A more extensive discussion of the method has been given in two earlier publications [25,26] (hereafter referred to as I and II). The present approach represents another basis-set method, with no explicit recourse to continuum orbitals, and there is no need for input of empirical data such as the threshold for ionization. The strength of the present method is its ability to make a comprehensive inclusion of true-correlation effects, in particular for the total cross section. Narrow resonances cannot, however, be reproduced, but the method should be well suited to predict broad shape resonances.

A main objective of the present investigation is also to

study the effects that different choices of independent-particle models will have on the many-body perturbation expansion. For the occupied orbitals the Hartree-Fock model represents a variationally optimized solution, whereas there is no such unique model potential for the excited states. Three different independent-particle potentials for the excited orbitals will be investigated: (i) the Hartree-Fock potential (V^N type of potential), (ii) a V^{N-1} type of potential where the excited states are obtained in the field of an ionic core with one valence electron removed. [this potential will be referred to as a V^{N-1} (II) potential], and (iii) a potential constructed in a more subtle way to yield approximations to the excited orbitals that would be obtained with the coupled Hartree-Fock model in the static case [this will also be a potential of V^{N-1} type, referred to as V^{N-1} (I)]. In addition results will also be presented for the "shifted" Hamiltonian, which is another special way of partitioning the Hamiltonian for the perturbation expansion (cf. I and II).

Computed total and partial photoionization cross sections are presented for the electronic ground state in CO at the fixed equilibrium internuclear separation. There has been a considerable interest in experimental photoionization studies of CO in the past [27-31], probably also stimulated by the interest in photoionization of CO adsorbed on solid surfaces. Several computations of CO cross sections have also been published, all of which are on the independent-particle level of accuracy [10,20,32,33].

II. THEORY

A. The dynamic polarizability

The total cross section for photoionization $\sigma(\omega)$ is obtained from the imaginary part $\text{Im}\alpha(\omega)$ of the complex polarizability $\alpha(\omega)$ through the well-known relation [34]

$$\sigma(\omega) = \frac{4\pi}{c} \omega \text{Im}\alpha(\omega). \quad (1)$$

In the present work the photoionization cross section is derived by inverting the simple integral equation (cf. I and II)

$$\alpha(i\eta) = \frac{c}{2\pi^2} \int_0^\infty \frac{\sigma(\omega)}{\eta^2 + \omega^2} d\omega, \quad (2)$$

The Hamiltonian H_0 and H' of Eq. (7) and the total Hamiltonian H are defined by

$$H_0 = \sum_{i=1}^N \left[-\frac{1}{2} \nabla_i^2 - \frac{Z_a}{r_{ia}} - \frac{Z_b}{r_{ib}} + V_l \right],$$

$$H' = \sum_{i < j} \frac{1}{r_{ij}} - \sum_{i=1}^N V_i,$$

$$H = H_0 + H', \quad (8)$$

where Z_a and Z_b indicate the charges of the two nuclei of

where $\alpha(i\eta)$ is the (real) polarizability computed for purely imaginary frequencies $i\eta$. Hence, by the present method the computational problem basically consists in calculating the dynamic polarizability $\alpha(\omega)$ on the imaginary frequency axis. The dynamic polarizability represents the linear response of an atomic or molecular system to an external electric field and is defined by the relation

$$\mathbf{p} = \alpha(\omega) \mathbf{F}, \quad (3)$$

where \mathbf{p} is the electric dipole moment, and \mathbf{F} is the applied external field. In the case of a diatomic molecule the well-known expression for $\alpha(\omega)$ takes the form [34,35]

$$\alpha_{\parallel}(\omega) = \alpha_z(\omega) = - \sum_{k (\neq n)} |\langle \psi_k | d_z | \psi_n \rangle|^2 \times \left[\frac{1}{E_n - E_k - \omega} + \frac{1}{E_n - E_k + \omega} \right], \quad (4)$$

where d_z denotes the component of the electric dipole moment of the molecule along the molecular axis. The expression for the perpendicular component $\alpha_{\perp}(\omega) = \alpha_x(\omega) = \alpha_y(\omega)$ is similar to that of Eq. (4) with d_z replaced by the perpendicular components d_x or d_y . For a freely rotating diatomic molecule the observable (real) polarizability will be an average over the three perpendicular molecule-fixed directions [35], i.e.,

$$\alpha(\omega) = \frac{1}{3} [2\alpha_{\perp}(\omega) + \alpha_{\parallel}(\omega)]. \quad (5)$$

To compute $\alpha(\omega)$ is a difficult problem since the eigenstates and energies of Eq. (4) are those of the total zero-field Hamiltonian of the system. In the present investigation the dynamic polarizability will be computed by use of many-body perturbation theory, as discussed in more detail in I. In the many-body linked-cluster expansion $\alpha(\omega)$ takes the form [36,37]

$$\alpha_z(\omega) = -(\langle \psi_0 | d_z | \psi_1^+ \rangle + \langle \psi_0 | d_z | \psi_1^- \rangle) / \langle \psi_0 | \psi_0 \rangle, \quad (6)$$

with

$$|\psi_1^\pm\rangle = \sum_L \frac{1}{E_0 - H_0 \mp \omega} H' \cdots \frac{1}{E_0 - H_0 \mp \omega} d_z \cdots \frac{1}{E_0 - H_0} H' |\phi_0\rangle. \quad (7)$$

the molecule. Only the electronic ground state is of current interest, and E_0 of Eq. (7) denotes the lowest eigenvalue of H_0 with corresponding eigenstate $|\Phi_0\rangle$. The linked-cluster expansion of Eq. (7) with no interaction with d_z yields the correct expression for the ground state $|\Psi_0\rangle$ of the total Hamiltonian H of Eq. (8).

B. Diagrammatic representation of $\alpha(\omega)$

The representation of the linked-cluster expansion of Eqs. (6) and (7) in terms of diagrams was discussed at

some length in I, and only a brief outline is reproduced here for the sake of completeness. A careful selection of the single-particle potentials V_i of Eq. (8) is of utmost importance for a successful many-body expansion. The potentials V_i determine the single-particle states $\varphi_n(\mathbf{r}_i)$ from the relation

$$\left[-\frac{1}{2}\nabla_i^2 - \frac{Z_a}{r_{ia}} - \frac{Z_b}{r_{ib}} + V_i \right] \varphi_n(\mathbf{r}_i) = \epsilon_n \varphi_n(\mathbf{r}_i). \quad (9)$$

For a diatomic molecule the standard procedure is to represent the single-particle states by analytic expansions in terms of a finite set of known basis functions. In this way the continuum is described by a finite set of virtual states. The Hartree-Fock potential V_{HF} is a favorite choice for the single-particle potentials. With that choice all the matrix elements of the effective potential V_{eff} defined by

$$\langle \varphi_k | V_{\text{eff}} | \varphi_l \rangle = \sum_{n=1}^N \langle \varphi_k \varphi_n | O | \varphi_l \varphi_n \rangle - \langle \varphi_k | V | \varphi_l \rangle \quad (10)$$

where

$$O = (1 - P_{12}) \frac{1}{r_{12}}$$

will vanish for a closed-shell system. Even for open-shell systems the Hartree-Fock potential will normally lead to rather insignificant contributions from V_{eff} . Hence, in particular for closed-shell systems the Hartree-Fock potential will lead to an extensive cancellation of terms in the perturbation expansion.

The perturbation expansions represented by Eqs. (6) and (7) are best visualized in terms of diagrams (cf. I). In the present work the expansion will be complete to second order in the Coulomb interaction H' of Eq. (8). Figure 1 displays the zero-order diagram, and the most important diagrams to first order in H' are shown in Fig. 2. The first-order diagrams are particularly interesting since they can be used to redefine the single-particle potentials, as discussed in II. It is well known that a double-perturbation expansion such as the present one is normally an inefficient approach to computing static polarizabilities ($\omega=0$). The coupled Hartree-Fock scheme is generally better for that purpose. Caves and Karplus [38] have studied the iterative solution of the coupled Hartree-Fock equations in terms of diagrams. They found that the zeroth iteration leads to the lowest-order diagram of Fig. 1, whereas the next iteration yields the first-order diagrams of Fig. 2. Hence, by choosing the single-particle potentials so that the sum of all the first-order diagrams of Fig. 2 vanishes in the static case (cf.

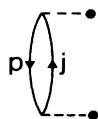


FIG. 1. Zeroth-order contribution to the dynamic polarizabilities $\alpha(\omega)$. The heavy dots indicate interactions with the dipole operator.

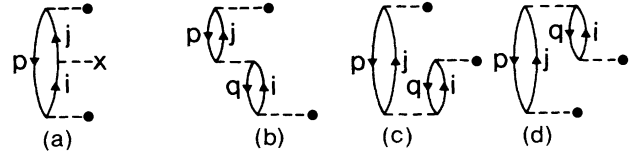


FIG. 2. Four most important first-order diagrams contributing to $\alpha(\omega)$. The cross represents interaction with the effective operator of Eq. (10).

II), the zero-order diagram in Fig. 1 should yield a fair approximation of the coupled Hartree-Fock result. This conclusion of course rests on the assumption that there is a fast convergence in the iterative solution to the coupled Hartree-Fock equations. Provided that assumption holds, the single-particle potentials constructed in this way should yield rapid convergence of the perturbation expansion. Such single-particle potentials also tend to be more attractive than the Hartree-Fock potentials (cf. II), and they will thereby resemble the V^{N-1} type of potentials. This is actually the V^{N-1} (I) potential mentioned in the Introduction.

C. Partial photoionization cross sections

The cross section $\sigma(\omega)$ obtained by inversion of Eq. (2) will certainly be the total cross section when $\alpha(i\eta)$ is the total polarizability computed for the whole system. Now, the inversion of Eq. (2) is a linear process, and partial cross sections may be derived, provided that the corresponding contributions to $\alpha(i\eta)$ can be identified.

The lowest-order diagram of Fig. 1 certainly yields separate contributions for excitation or ionization from the distinct occupied orbitals. The same conclusion applies in the next order to the diagrams of Figs. 2(a), 2(c), and 2(d). From the diagram of Fig. 2(b) the contribution to the z component of $\alpha(i\eta)$ takes the form [cf. Eqs. (9) and (10)]

$$\alpha_z^\pm(i\eta) = - \sum_{p,q} \sum_{i,j} \frac{\langle p | d_z | j \rangle \langle jq | 0 | pi \rangle \langle i | d_z | q \rangle}{(\epsilon_p - \epsilon_j \pm i\eta)(\epsilon_q - \epsilon_i \pm i\eta)}, \quad (11)$$

and there is a combined contribution from the occupied orbital p as well as the orbital q .

Now, separate contributions from electrons in different shells may be obtained from Eq. (11) by transforming those terms where p and q refer to electrons in different shells, i.e., $\epsilon_p \neq \epsilon_q$. A simple partial fraction decomposition for the terms of Eq. (11) with $\epsilon_p \neq \epsilon_q$ leads to

$$\begin{aligned} \alpha_z^\pm(i\eta) = & - \sum_{p,q} \sum_{i,j} \frac{\langle p | d_z | j \rangle \langle jq | O | pi \rangle \langle i | d_z | q \rangle}{(\epsilon_p - \epsilon_j \pm i\eta)(\epsilon_q - \epsilon_i \pm i\eta)} \\ & - 2 \sum_{p,j} \frac{\langle p | d_z | j \rangle}{\epsilon_p - \epsilon_j \pm i\eta} \sum_{q,i}' \frac{\langle jq | O | pi \rangle \langle i | d_z | q \rangle}{(\epsilon_q - \epsilon_i) - (\epsilon_p - \epsilon_j)}, \end{aligned} \quad (12)$$

where the prime on the first summation means that only terms with $\epsilon_p = \epsilon_q$ are included, whereas the double prime on the summation over q and i means that terms with $\epsilon_p = \epsilon_q$ are excluded.

Now, the first part of Eq. (12) yields the contribution from the different shells from interactions within the relevant shell only, whereas the second part in principle yields the contributions from individual occupied orbitals p from intershell interactions ($\epsilon_p \neq \epsilon_q$). In practice difficulties may arise in the evaluation of the second part of Eq. (12). There may accidentally be denominators in the summation over q and i that will nearly vanish even though ϵ_p is different from ϵ_q and there is a summation over just a finite set of discrete orbital energies ϵ_i and ϵ_j . This problem is in particular relevant for molecules where the orbital energies of different shells may come quite close. Working with continuum orbitals and integration over continuous orbital energies this problem is handled by principal-value integration [39]. By the present method in which the continuum is represented through a finite set of virtual orbitals a few singular terms in the second part of Eq. (12) may have to be omitted. In practice this is accomplished by adding a small imaginary quantity to the denominators in the summation over q and i and then exploring the real part of the sum as the added imaginary quantity tends to zero. In the case of irregularities one may have to use the real value of the sum for a finite small value of the added imaginary quantity. Such singularities are obviously related to a specific choice of the single-particle potentials (cf. Sec. II B), and the singularities will be removed or shifted by another choice of potentials. Hence, there is an opportunity to test the consistency of the present procedure by different choices of potentials.

The contributions to the partial cross sections from intershell interactions to second order are obtained by a procedure similar to that described above for the first-order diagram of Fig. 2(b). However, whereas the possible first-order singularities of the first-order diagram of Fig. 2(b) are rather straightforward to handle, the second-order diagrams may lead to second-order singularities that need a particularly careful treatment.

The inversion of Eq. (2) proceeds as described in I. The cross section is expanded in a finite set of known functions $\psi_n(\omega)$.

$$\sigma(\omega) = \sum_a a_n \psi_n(\omega), \quad (13)$$

with

$$\psi_n(\omega) = S(\omega - \omega_0) \omega^3 e^{-k_n \omega}, \quad (14)$$

and

$$k_n = k_0 C^{n-1}. \quad (15)$$

In Eq. (14) $S(\omega - \omega_0)$ is a unit step function that ensures that $\sigma(\omega) = 0$ for $\omega < \omega_0$. Use of the step function may reduce the number of terms needed in Eq. (13). If needed, the step function will in practice be made smooth so that it gradually increases from zero to 1 over a range of frequencies around ω_0 . k_0 and C ($C > 1$) of Eq. (15) are real constants to be adjusted for an optimal solution of Eq. (2).

The computed values of $\sigma(\omega)$ yield the real part of the polarizability $\text{Re}\alpha(\omega)$ on the real axis through the

Kramers-Kronig dispersion relation [40]

$$\text{Re}\alpha(\omega) = \frac{c}{2\pi^2} \text{P} \int_0^\infty \frac{\sigma(\omega')}{\omega'^2 - \omega^2} d\omega'. \quad (16)$$

$\text{Re}\alpha(\omega)$ gives information on important optical properties such as the index of refraction.

III. COMPUTED RESULTS

A. The dynamic polarizability $\alpha(i\eta)$

The dynamic polarizability $\alpha(i\eta)$ has been computed for the ground state in CO by use of many-body perturbation theory as outlined in Sec. II B. All computations were carried out for the fixed internuclear separation $R = R_e = 2.132$ a.u. The basis sets used for the present calculations were extensions of the sets of Slater atomic orbitals with optimized exponents published by Cade and Huo [41]. With the orbital exponent in parentheses, the specific extensions are as follows: $\sigma 2s_c$ (0.60), $\sigma 2s_o$ (0.90), $\sigma 2p_c$ (0.60), $\sigma 2p_o$ (0.80), $\pi 2p_c$ (0.80), $\pi 2p_o$ (0.80), $\pi 3d_c$ (0.50), $\pi 3d_o$ (0.80), $\pi 3d_o$ (0.50), $\pi 3d_o$ (0.80). In addition a set of seven δ orbitals were included, based on three $3d$ orbitals on C with exponents 0.50, 0.85, and 1.45, and four $3d$ orbitals on O with exponents 0.50, 0.85, 1.45, and 2.45. A few tests were made with slightly larger basis sets (more diffuse orbitals), without obtaining significant changes in the computed results.

Computed values of $\alpha(i\eta)$ are given in Table I for a few selected η values. Hartree-Fock potentials were used, and the perturbation expansion is complete to second order in the Coulomb interaction H' of Eq. (8). The static polarizability obtained for $\eta = 0$ may be compared with experimental results as well as other theoretical predictions. The most recent theoretical values seem to be those of Rerat *et al.* [42], and they find $\alpha_z(0) = 14.96$ a.u. when their configuration interaction approach is combined with an extrapolation method. Kellö *et al.* [43] obtained $\alpha_z(0) = 15.07$ a.u. from a finite field method combined with a perturbation expansion to fourth order. The experimental value is 15.72 a.u. [44]. The present result from Table I is $\alpha_z(0) = 14.15$ a.u., and thus about 5% lower than the other most refined theoretical values. A characteristic feature of Table I is the slow convergence for $\alpha_z(0)$. Another characteristic feature is, however, the rapid increase in the convergence with increasing values of η .

For the perpendicular component the theoretical value of Rerat *et al.* is $\alpha_x(0) = 11.25$ a.u., whereas the experimental result is 12.15 a.u. [44]. The present result $\alpha_x(0) = 9.91$ a.u. is thus in rather modest agreement with the experimental value. Similar to $\alpha_z(0)$ the rate of convergence for $\alpha_x(0)$ is seen to be rather poor, however, with rapid improvement for increasing η . Thus, the present results are in agreement with the general conclusion that a double perturbation expansion based on zero-field single-particle states yields an inefficient approach to computing static polarizabilities. However, the cross section $\sigma(\omega)$ is through Eq. (2) determined from $\alpha(i\eta)$ for a larger range of η values where the convergence is quite fast. Hence, accurate cross sections may be

TABLE I. Computed values of $\alpha(i\eta)$ (in a.u., 1 a.u.=0.1482 Å³) for the ground state of CO at $R=2.132$ a.u.

η	z component, order				x component, order			
	0	1	2	Total	0	1	2	Total
0.00	12.30	-2.23	4.08	14.15	9.072	0.477	0.359	9.91
0.30	10.97	-2.31	2.90	11.56	8.129	-0.109	0.014	8.03
0.60	8.414	-2.16	1.26	7.51	6.341	-0.752	-0.201	5.39
1.00	5.602	-1.65	0.232	4.18	4.366	-0.906	-0.173	3.29
2.00	2.362	-0.777	-0.148	1.43	1.972	-0.559	-0.083	1.33
4.00	0.7656	-0.270	-0.082	0.414	0.682	-0.212	-0.035	0.435
8.00	0.217	-0.078	-0.027	0.112	0.202	-0.063	-0.013	0.126

obtained, even though the static polarizabilities are in modest agreement with experiment.

Table II lists static polarizabilities obtained with the two different V^{N-1} types of potential mentioned in the Introduction, in addition to those computed with the Hartree-Fock potential. V^{N-1} (I) is a potential based on a partial cancellation of the diagrams of Fig. 2, as discussed in Sec. II B. A full cancellation could not be achieved due to a considerable σ - π interaction in the diagrams of Figs. 2(b)–2(d), in particular in diagrams (c) and (d). The total result to second order obtained with the V^{N-1} (I) potential is only in slightly better agreement with experiment, whereas the lowest-order result (11.30 a.u.) for $\alpha_x(0)$ represents a substantial improvement compared with that of the Hartree-Fock potential.

The V^{N-1} (II) potential is a more standard V^{N-1} type of potential obtained from a partial cancellation of the diagrams of Figs. 2(a) and 2(b), with neglect of the σ - π interaction in diagram (b). Compared with the V^{N-1} (I) potential the V^{N-1} (II) one is more attractive. With the V^{N-1} (II) potential the excited (virtual) states are obtained with either one 5σ or one π electron removed, depending on the component of $\alpha(i\eta)$ and the symmetry of the excited orbital. From Table II it is clear that the V^{N-1} (II) potential to lowest order yields results for $\alpha_z(0)$ as well as $\alpha_x(0)$ that are quite impressive compared with the experimental values of 15.72 and 12.15 a.u., respectively. The convergence of the perturbation expansion for this potential is, unfortunately, poor, in particular for $\alpha_z(0)$, and the second-order result for $\alpha_x(0)$ is inferior to those obtained with the other potentials. Thus, the V^{N-1} (II) potential represents an accurate effective potential for an independent-particle model, but it is unphysical in the sense that it does not provide a useful

basis for a perturbation expansion. Similar arguments obviously also apply to the results obtained with the shifted Hamiltonian (cf. I and II). This is another way of partitioning the total zero-field Hamiltonian to create an effective potential that is quite similar to the V^{N-1} (II) potential.

Various other V^{N-1} types of potentials were tried, normally with divergent results for $\alpha_z(0)$ caused by large contributions from the effective potential of Eq. (10). The problems encountered in computing $\alpha_z(0)$ tend to stem from the Rydberg character of all the five lowest excited $^1\Sigma$ states in CO, as pointed out by Rerat *et al.* [42].

In view of the failure to find a V^{N-1} type of potential that could give improvements compared with the Hartree-Fock potential that are substantial for α_z as well as α_x , it was decided to make use of the Hartree-Fock potential. An important argument in favor of that decision is also that the effective potential of Eq. (10) vanishes for the Hartree-Fock single-particle potential.

B. Dynamic polarizabilities related to partial cross sections

Tables III and IV list dynamic polarizabilities that can be related to excitation or ionization from the 1π , 5σ , 4σ , and 3σ shells respectively. As discussed in Sec. II C, the first-order diagram of Fig. 2(b) makes a combined contribution to the cross sections for orbitals p and q , and the separate contributions were obtained from Eq. (12). Separate contributions related to the various orbitals are harder to extract from the second-order diagrams (see I for examples of second-order diagrams). For some of the diagrams to that order the separation process leads to terms that are nearly singular, and where the singularity is of second order. These terms had to be omitted, lead-

TABLE II. Static polarizability $\alpha(0)$ (in a.u.) for CO computed for three different potentials with a standard (Möller-Plesset) partitioning of the Hamiltonian, and for a V^N (Hartree-Fock) potential for the shifted (Epstein-Nesbet) partitioning (cf. text).

Potential	z component, order				x component, order			
	0	1	2	Total	0	1	2	Total
V^N (HF)	12.30	-2.23	4.08	14.15	9.07	0.48	0.36	9.91
V^{N-1} (I)	12.86	-1.76	3.46	14.56	11.30	-2.39	1.10	10.01
V^{N-1} (II)	15.00	-5.70	7.45	16.75	12.34	-5.16	1.99	9.17
Shifted V^N (HF)	16.23	-8.88	11.55	18.90	11.99	-3.10	1.08	9.97

TABLE III. z component of $\alpha(i\eta)$ (in a.u.) that corresponds to absorption or ionization from the various listed orbitals.

Orbital	η	V^N potential, order				V^{N-1} (II) potential, order			
		0	1	2	Total	0	1	2	Total
π	0.00	8.04	-4.94	4.30	7.40	9.25	-7.42	6.81	8.64
	1.00	3.22	-2.52	1.42	2.12	3.02	-2.54	1.78	2.26
	4.00	0.34	-0.31	0.14	0.17	0.30	-0.26	0.15	0.19
5σ	0.00	3.09	2.62	-1.32	4.39	4.40	2.12	-1.73	4.79
	1.00	1.54	0.76	-1.01	1.29	1.46	0.82	-0.91	1.37
	4.00	0.21	0.035	-0.14	0.11	0.15	0.086	-0.11	0.13
4σ	0.00	1.02	0.47	-0.13	1.36	1.21	0.51	-0.78	0.94
	1.00	0.72	0.26	-0.14	0.84	0.74	0.29	-0.48	0.55
	4.00	0.16	0.023	-0.029	0.15	0.14	0.043	-0.083	0.10
3σ	0.00	0.14	0.037	0.065	0.24	0.15	0.043	0.12	0.31
	1.00	0.12	0.024	0.055	0.20	0.13	0.031	0.10	0.26
	4.00	0.044	-0.003	0.021	0.062	0.041	0.003	0.035	0.079

ing to an approximate inclusion of the second-order corrections that stem from intershell interactions. This will in particular turn out to affect the 4σ and 5σ cross sections due to strong 4σ - 5σ interactions.

A prominent feature of Table III is the slow convergence for the z component of $\alpha(i\eta)$. For the most attractive V^{N-1} (II) potential the perturbation expansion through the three lowest orders yields oscillating terms with very slow convergence. For the V^N potential the situation is somewhat better, but the contributions from the second-order terms are also in this case too high for a satisfactory termination of the perturbation expansion to that order.

However, the results of Table IV show that the situation is significantly better for the x component of $\alpha(i\eta)$, which also yields the major contribution to the cross sections. The best rate of convergence for the x component is obtained for the V^N potential, and that was also the case for the z component.

The second-order terms make important contributions to $\alpha(i\eta)$, as pointed out above. Furthermore, it is of in-

terest to note that triple excitations, which are normally neglected in many-body photoionization computations, are found to make substantial second-order contributions. From other areas of many-body work it is known that quadruple excitations are often more important than triple excitations. This might certainly be the case also for photoionization, and a major source of inaccuracies in the present many-body results could be the lack of quadruple excitations which do not occur to second order.

C. The total photoionization cross section

The computed total photoionization cross section for the ground state in CO at $R = R_e = 2.132$ a.u. is given in Table V and displayed in Fig. 3. The (real) isotropic polarizability

$$\alpha(i\eta) = \frac{1}{3}[2\alpha_{\perp}(i\eta) + \alpha_{\parallel}(i\eta)] \quad (17)$$

was computed at 22 η values in the range $\eta=0.0$ to 12.0 a.u. (cf. Table I), and the discrete values were fitted to a series of exponentials to obtain a smooth and continuous

TABLE IV. x component of $\alpha(i\eta)$ (in a.u.) that corresponds to absorption or ionization from the various listed orbitals.

Orbital	η	V^N potential, order				V^{N-1} (II) potential, order			
		0	1	2	Total	0	1	2	Total
π	0.00	3.92	0.46	0.32	4.70	4.82	-0.70	0.67	4.79
	1.00	2.20	-0.24	-0.039	1.92	1.95	-0.34	0.25	1.86
	4.00	0.36	-0.11	0.004	0.25	0.26	-0.085	0.053	0.23
5σ	0.00	3.62	-0.19	0.36	3.79	5.51	-3.70	0.23	2.04
	1.00	1.32	-0.58	-0.055	0.69	0.96	-0.36	0.013	0.61
	4.00	0.16	-0.069	0.0009	0.092	0.11	-0.020	-0.019	0.069
4σ	0.00	1.47	0.27	0.21	1.95	1.94	-0.79	1.66	2.81
	1.00	0.79	-0.071	0.053	0.77	0.67	-0.13	0.49	1.03
	4.00	0.12	-0.033	0.029	0.12	0.087	0.024	0.066	0.18
3σ	0.00	0.059	-0.012	-0.009	0.038	0.060	0.022	-0.024	0.058
	1.00	0.053	-0.011	-0.006	0.036	0.053	0.019	-0.015	0.057
	4.00	0.024	-0.008	0.001	0.017	0.021	0.009	0.0006	0.031

TABLE V. Computed total and partial absorption (ionization) cross sections (Mb) to second order by use of the Hartree-Fock single-particle potential (V^N).

ω (a.u.)	$1\pi^{-1}$	$5\sigma^{-1}$	$4\sigma^{-1}$	$3\sigma^{-1}$	Sum of partials	Total $\sigma(\omega)$
0.25	0.12	1.58	0.00		1.70	1.53
0.30	2.01	3.10	0.16		5.27	5.22
0.35	4.34	4.63	0.49		9.46	9.58
0.40	6.73	5.95	0.92		13.60	13.93
0.50	10.70	7.57	1.95		20.22	20.87
0.60	13.00	7.81	2.97		23.78	24.60
0.70	13.81	7.12	3.81		24.74	25.51
0.80	13.59	5.98	4.41		23.98	24.58
0.90	12.80	4.75	4.79		22.34	22.67
1.00	11.74	3.62	4.98		20.34	20.38
1.10	10.61	2.68	5.03		18.32	18.05
1.20	9.50	1.93	4.97		16.40	15.87
1.40	7.51	0.96	4.66	0.14	13.27	12.15
1.60	5.86	0.46	4.22	0.70	11.24	9.26
1.80	4.51	0.21	3.73	1.04	9.49	7.01
2.00	3.42	0.10	3.25	1.19	7.96	5.27
2.50	1.59	0.02	2.17	1.10	4.88	2.43
3.00	0.67		1.34	0.79	2.80	1.02
4.00	0.10		0.42	0.33	0.85	0.15

representation of $\alpha(i\eta)$. In the next step the cross section $\sigma(\omega)$ was obtained by inverting Eq. (2), as briefly discussed in Sec. II C (cf. I). A set of four basis functions $\psi_n(\omega)$ [cf. Eq. (13)] was found to be sufficient, based on the parameters $k_0=2.8$ and $C=2.0$ of Eq. (15). The step function $S(\omega-\omega_0)$ of Eq. (14) was not needed. The present way of computing the cross section yields a continuous curve which is actually a measure for the total absorption coefficient. Thus, there should be a zero result for frequencies below the first excitation energy which is 0.296 a.u. in the present case ($A^1\Pi$ state). The photoionization cross section is obtained for frequencies above the

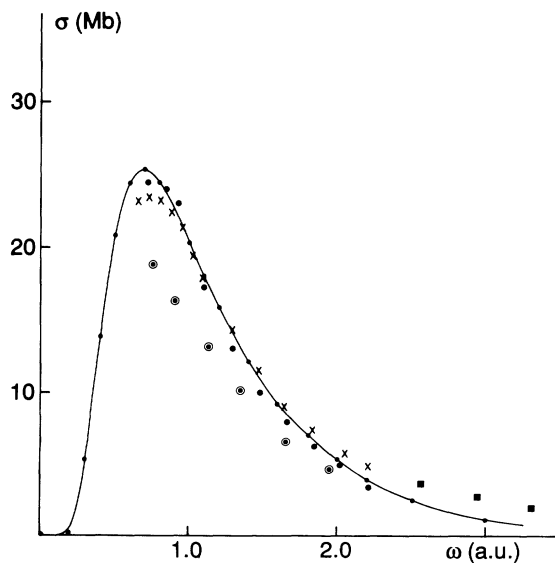


FIG. 3. Computed total absorption (photoionization) cross section for CO. —, present results; ●, Padial *et al.* [10]; ○, Davenport [32]; ×, experiment [28]; ■, experiment [31].

ionization threshold of 0.515 a.u.

From Fig. 3 the present results to second order in the many-body expansion are seen to be in good agreement with experimental values [28,31], as well as with the results of Padial *et al.* [10] obtained with the separated-channel static-exchange approximation. The good agreement between the present many-body results and those of Padial *et al.*, which are actually based on a rather rough independent-particle model, is quite remarkable. The present results clearly indicate that higher-order effects are important in the computation of $\alpha(i\eta)$, in particular the first-order ones, and also that the results to lowest order will depend very much on the chosen single-particle potentials. Thus, the static-exchange frozen-core potentials of V^{N-1} type used by Padial *et al.* for their independent-particle model seem to be a very fortunately choice for CO.

The independent-particle results of Davenport [32] obtained with the scattered wave (SW) $X\alpha$ method (local potentials) are also shown in Fig. 3. This independent-particle method clearly does not make very accurate predictions of the total cross section.

Figure 4 shows the dispersion curve $\text{Re}\alpha(\omega)$ obtained from Eq. (16) and the computed values of $\sigma(\omega)$. Characteristic features of the dispersion curve are the maximum close to the excitation energy 0.296 a.u. of the lowest excited state ($A^1\Pi$), and the free-electron behavior $-n/\omega^2$ for the higher frequencies, where n is the number of “free” electrons.

D. Partial cross sections

Computed partial cross sections related to the 1π , 5σ , 4σ , and 3σ shells are visualized in Figs. 5–9, and numerical values are given in Table V. The cross sections were derived from Eq. (2) and the computed parts of $\alpha(i\eta)$ that are pertinent to the relevant shell, as discussed in Secs. II C and III B.

Figure 5 displays the partial cross section for ionization from the 1π shell, which is also the dominant partial

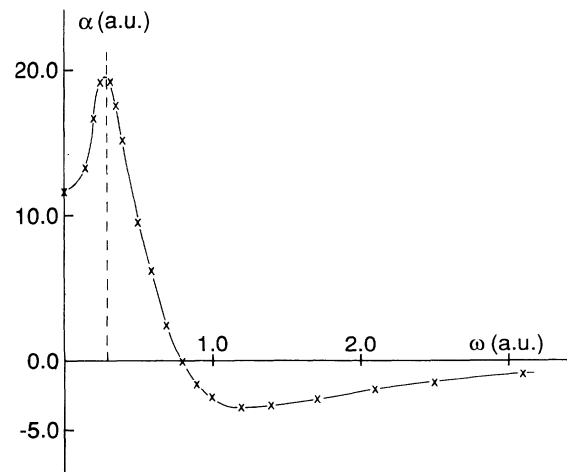


FIG. 4. Dispersion curve [real part of $\alpha(\omega)$ on the real frequency axis] for CO. The vertical dashed line indicates the energy (0.296 a.u.) of the first excited $A^1\Pi$ state.

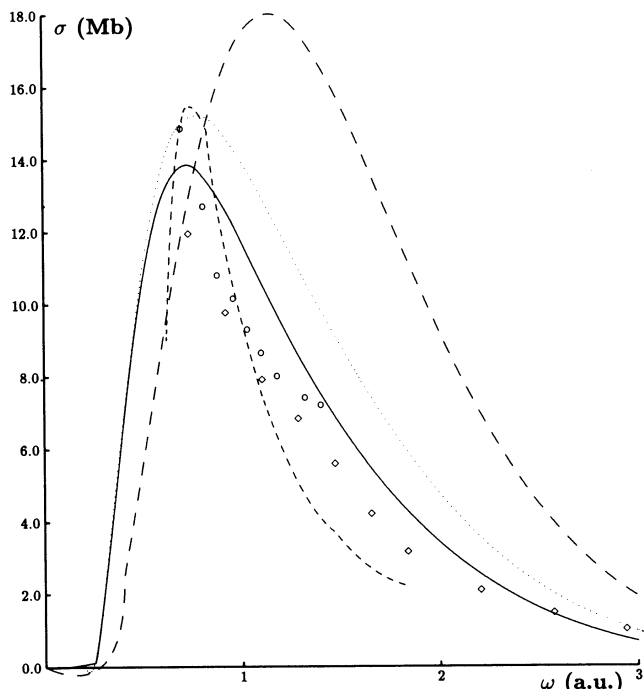


FIG. 5. Partial cross section for 1π ionization. Solid line, second order V^N ; long dashes, lowest order V^N ; dotted, lowest order V^{N-1} (II); short dashes, Padial *et al.* [10]; ○, experiment [27]; ◇, experiment [31].

cross section in CO. The agreement with experiment for the present results based on a perturbation expansion to second order and a V^N potential (solid line) is quite good. Figure 5 also clearly visualizes how the computed results are substantially improved in going from the lowest order (long dashes) to the second order in the perturbation expansion. The dotted curve represents the partial cross

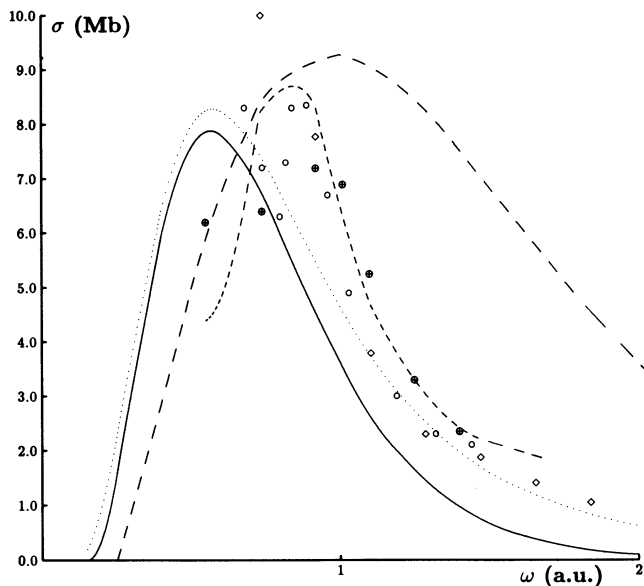


FIG. 6. Partial cross section for 5σ ionization. Solid line, second order V^N ; long dashes, lowest order V^N ; dotted, lowest order V^{N-1} (II); short dashes, Padial *et al.* [10]; ⊕, Lucchese and McKoy [20]; ○, experiment [27]; ◇, experiment [31].

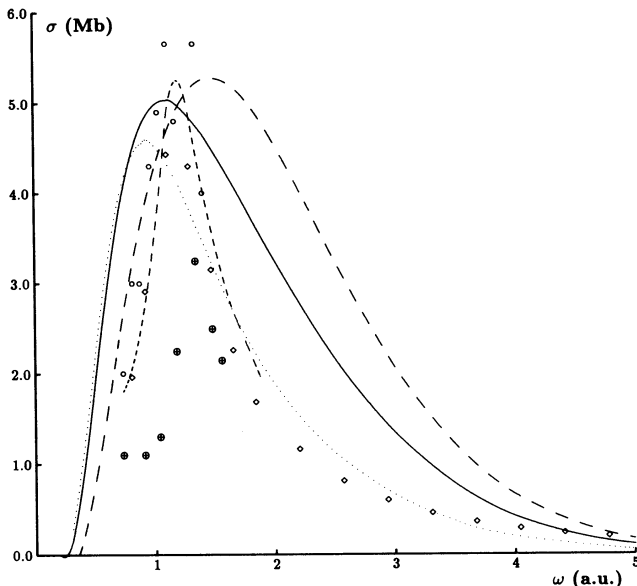


FIG. 7. Partial cross section for 4σ ionization. Solid line, second order V^N ; long dashes, lowest order V^N ; dotted, lowest order V^{N-1} (II); short dashes, Padial *et al.* [10]; ⊕, Davenport [32]; ○, experiment [27], ◇, experiment [31].

section obtained with the most attractive V^{N-1} (II) potential to lowest order in the perturbation expansion. Thus, to lowest order the V^{N-1} potential yields much better agreement with experiment than the V^N potential, but the perturbation expansion based on the V^{N-1} potential is very slowly convergent (cf. Tables III and IV), and higher-order corrections based on that potential will accordingly be quite unreliable. The independent-particle

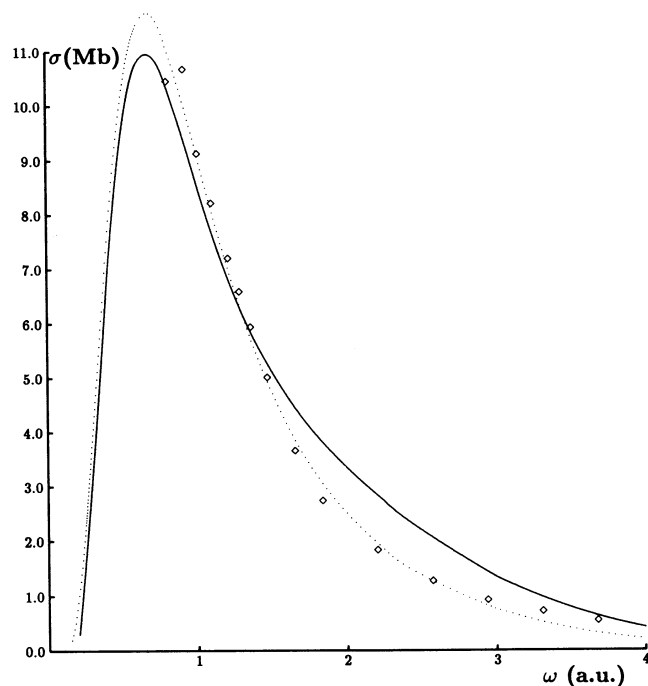


FIG. 8. Sum of partial cross sections for 4σ and 5σ ionization. Solid line, second order V^N ; dotted, lowest order V^{N-1} (II); ◇, experiment [31].

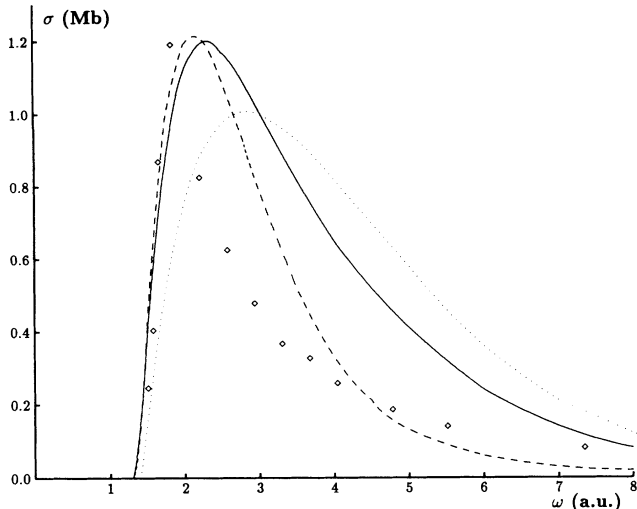


FIG. 9. Partial cross sections for 3σ ionization. Solid line, second order V^N ; dashes, first order V^N ; dotted, lowest order V^N ; \diamond , experiment [31].

predictions of Padiál *et al.* [10] based on a V^{N-1} potential are also shown in Fig. 5 (short dashes) and are seen to be in reasonable agreement with the present results.

Partial cross sections for ionization from the 5σ and 4σ shells are shown in Figs. 6 and 7, respectively. For the 5σ cross section a considerable improvement compared with experiment is obtained in going from the lowest order (long dashes) to the second order (solid line) for the V^N potential. There are, however, still significant disagreements between the present second-order results and the observed values, as might be expected in view of the poor convergence for the z component of $\alpha(i\eta)$ in this case (cf. Table III). The best agreement with experiment is obtained with the attractive V^{N-1} (II) potential to lowest order (dotted line), but severe convergence problems in the perturbation expansion for the z component as well as the x component of $\alpha(i\eta)$ (cf. Tables III and IV) yield highly unreliable higher-order corrections in this case. Figure 6 also includes the computed independent-particle results of Padiál *et al.* [10] and the more refined independent particle (Hartree-Fock) single-center results of Lucchese and McKoy [20]. It is quite interesting to note that of those two independent-particle models the most refined one of Lucchese and McKoy clearly makes predictions that are inferior to those of the simpler model of Padiál *et al.*

For the 4σ cross section shown in Fig. 7 the improvement obtained by going from the lowest order to second order is less substantial than for the 1π and 5σ cross sections. The convergence of the perturbation expansion is also in this case quite slow, and there remain significant disagreements between the present second-order results obtained with the V^N potential and the observed values. Very good agreement with experiment is, however, obtained with the V^{N-1} (II) potential to lowest order (dotted line). The convergence of the perturbation expansion for the V^{N-1} (II) potential is, unfortunately, as for the 1π and 5σ shells, very poor, and reliable higher-order corrections based on the V^{N-1} (II) potential are unattain-

able. Also in this case are the independent-particle results of Padiál *et al.* [10] in good agreement with experiment, whereas the SW ($X\alpha$) values of Davenport [32] obtained with a local potential are hardly even in qualitative agreement with the experimental results.

In Fig. 8 are shown experimental and theoretical values for the sum of the 4σ and 5σ partial cross sections. As expected from Figs. 6 and 7 the lowest-order predictions based on the V^{N-1} (II) potential are in excellent agreement with observations. What is more interesting, however, is that the second-order results obtained with the V^N potential for this sum is also in very good agreement with experiment. The reason why the sum is much better predicted than the individual 4σ and 5σ cross sections is clearly related to the strong interaction between the 4σ and 5σ shells, which pushes the related polarizabilities strongly in opposite directions. Thus, the sum of the cross sections can be obtained very well from a perturbation expansion, whereas the individual ones are hard to describe in a perturbative manner.

Finally, the computed partial cross section for the 3σ shell shown in Fig. 9 is seen to be in excellent agreement with the observed values for low frequencies. For higher frequencies the first-order prediction (dashed curve) is seen to be in best agreement with experiment, and the largest deviation from experiment is found to lowest order (dotted line). Here again the convergence of the perturbation series is slow due to large interaction with the 4σ and 5σ shells. The results shown in Fig. 9 were obtained with the V^N potential which to lowest order yields results quite identical to those of the V^{N-1} (II) potential (cf. Tables III and IV). The convergence of the perturbation expansion based on the V^{N-1} potential is, however, also in this case clearly inferior to that based on the V^N potential.

A final comment should be added to Table V. For the lower frequencies up to about 1.40 a.u. there is good or fair agreement between the total cross section and the sum of the partial ones. At higher frequencies the sum tends to be somewhat larger than the total cross section. This discrepancy mainly arises from the approximations made in the second-order corrections for the polarizabilities used to determine the partial cross sections. Inaccuracies in the computed $\alpha(i\eta)$ values will through the numerical inversion of Eq. (2) in particular lead to rather large relative errors in the small $\sigma(\omega)$ values for high frequencies.

IV. CONCLUDING REMARKS

The present method to compute photoionization cross sections from a many-body expansion for the (real) dynamic polarizability $\alpha(i\eta)$ on the imaginary axis tends to work quite well for the total cross section. For low η values the rate of convergence may seem slow, and the static polarizabilities obtained are in rather modest agreement with experiment. However, the rate of convergence improves very fast with increasing η values, and the computation of $\sigma(\omega)$ from $\alpha(i\eta)$, which is based on a broad range of η values, should be a sound procedure. Another familiar problem to be underlined is the high sensitivity of the computed results to the single-particle potentials.

Among the potentials tested in Table II the so-called shifted Hamiltonian actually represents an attractive V^{N-1} potential that is seen to yield excellent results for the static polarizability to lowest order. However, this potential is nonetheless quite ill-behaved as there is no convergence to second order in the perturbation expansion for $\alpha_z(0)$. To overcome the rather arbitrary dependence on the potential, the calculation certainly has to be carried beyond the independent-particle level of accuracy (lowest order). The results of the V^N (HF) and V^{N-1} (I) potentials of Table II illustrate this point quite well. Those potentials do not necessarily yield accurate or close results to lowest order, but they lead to reasonable convergencies of the perturbation expansion, and to second order the results come quite close.

For the partial cross sections the present method suffers from the same deficiency as other basis-set methods in that extra approximations have to be made. The present results, however, indicate that the effect of the extra approximations are of minor importance compared with those arising from the termination of the perturbation expansion, even when it is brought to the second order.

A general conclusion would be that the theoretical handling of the many-body effects involved in photoionizing a molecule like CO is far from a straightforward process. First of all the choice of independent-particle potential is crucial. The V^{N-1} (II) potential, which is expected to yield a reasonable representation of the potential affecting the outgoing electron, is found to make quite accurate predictions of the cross sections to the lowest order in the perturbation expansion. However, large and hardly convergent higher-order terms result by use of that potential. Thus, the V^{N-1} (II) potential mere-

ly represents a rather accurate phenomenological independent-particle description of the ionization process in CO. The Hartree-Fock (V^N) potential on the other hand yields poor lowest-order results, but the perturbation expansion based on that potential tends to be convergent, although too slowly to lead to accurate second-order results for some of the partial cross sections.

Correlation effects are normally identified as corrections to the results obtained with an independent-particle model. The variationally optimized Hartree-Fock model is generally accepted as the best independent-particle description of the occupied orbitals. However, computed photoionization properties are very sensitive to the quality of the excited continuum orbitals used, and for the excited orbitals, there is, unfortunately, no such unique independent-particle model. Thus, it may be hard to identify well-defined correlation effects and many-body effects in photoionization work. For atoms with weak interactions between the different shells it is possible to identify a unique and efficient V^{N-1} type of model where the excited orbitals are obtained in a potential with one valence electron removed. This situation also tends to apply to hydrides like OH and HF, and explains why a V^{N-1} potential was found to be superior to the Hartree-Fock potential in those molecules (cf. II), contrary to the present results for CO. In the case of CO no unique V^{N-1} potential could be obtained due to the strong interactions between the 4σ , 5σ , and 1π valence shells.

ACKNOWLEDGMENTS

The author is greatly indebted to O. Hemmers and U. Becker for stimulating comments on the present work and for making their experimental results on CO available prior to publication.

-
- [1] M. Ya. Amusia and N. A. Cherepkov, *Case Stud. At. Phys.* **5**, 47 (1975).
- [2] A. F. Starace, in *Corpuscles and Radiation in Matter I*, edited by W. Mehlhorn, *Handbuch der Physik* Vol. 31 (Springer, Berlin, 1980).
- [3] H. P. Kelly, *Phys. Scr. T* **17**, 109 (1987).
- [4] P. W. Langhoff and C. T. Corcoran, *J. Chem. Phys.* **61**, 146 (1974).
- [5] P. W. Langhoff, C. T. Corcoran, J. S. Sims, F. Weinhold, and R. M. Glover, *Phys. Rev. A* **14**, 1042 (1976).
- [6] J. T. Broad and W. P. Reinhardt, *Chem. Phys. Lett.* **37**, 212 (1976).
- [7] T. N. Rescigno, C. F. Bender, B. V. McKoy, and P. W. Langhoff, *J. Chem. Phys.* **68**, 2992 (1978).
- [8] I. Cacelli, V. Carravetta, and R. Moccia, *J. Phys. B* **18**, 1375 (1985).
- [9] I. Cacelli, V. Carravetta, and R. Moccia, *Mol. Phys.* **59**, 385 (1986).
- [10] N. Padiyal, G. Csanak, B. V. McKoy, and P. W. Langhoff, *J. Chem. Phys.* **69**, 2992 (1978).
- [11] T. N. Rescigno, C. F. Bender, B. V. McKoy, and P. W. Langhoff, *J. Chem. Phys.* **68**, 970 (1978).
- [12] J. T. Broad and W. P. Reinhardt, *J. Chem. Phys.* **60**, 2182 (1974).
- [13] T. N. Rescigno, C. W. McCurdy, Jr., and V. McKoy, *Phys. Rev. A* **9**, 2409 (1974).
- [14] P. H. S. Martin, T. N. Rescigno, and V. McKoy, *Chem. Phys. Lett.* **29**, 496 (1974).
- [15] S. Yabushita, C. W. McCurdy, and T. N. Rescigno, *Phys. Rev. A* **36**, 3146 (1987).
- [16] T. E. H. Walker and H. P. Kelly, *Chem. Phys. Lett.* **16**, 511 (1972).
- [17] K. Faegri, Jr. and H. P. Kelly, *Phys. Rev. A* **23**, 52 (1981).
- [18] R. R. Lucchese, G. Raseev, and V. McKoy, *Phys. Rev. A* **25**, 2572 (1982).
- [19] J. A. Stephens and V. McKoy, *J. Chem. Phys.* **88**, 1737 (1988).
- [20] R. R. Lucchese and V. McKoy, *Phys. Rev. A* **28**, 1382 (1983).
- [21] R. R. Lucchese and R. W. Zurales, *Phys. Rev. A* **44**, 291 (1991).
- [22] M. T. Lee, J. A. Stephens, and V. McKoy, *J. Chem. Phys.* **92**, 536 (1990).
- [23] L. Ackermann, A. Görling, and N. Rösch, *J. Phys. B* **23**, 2485 (1990).
- [24] A. J. Sadlej, *J. Chem. Phys.* **75**, 320 (1981).
- [25] L. Veseth, *Phys. Rev. A* **44**, 358 (1991).
- [26] L. Veseth and H. P. Kelly, *Phys. Rev. A* **45**, 4621 (1992).
- [27] E. W. Plummer, T. Gustafsson, W. Gudat, and D. E. Eastman, *Phys. Rev. A* **15**, 2339 (1977).
- [28] G. R. Wight, M. J. Van der Wiel, and C. E. Brion, *J. Phys. B* **9**, 675 (1976).

- [29] A. Hamnett, W. Stoll, and C. E. Brion, *J. Electron Spectrosc. Relat. Phenom.* **8**, 367 (1976).
- [30] J. A. R. Samson and J. L. Gardner, *J. Electron Spectrosc. Relat. Phenom.* **8**, 35 (1976).
- [31] O. Hemmers (private communication).
- [32] J. W. Davenport, *Phys. Rev. Lett.* **36**, 945 (1976).
- [33] A. Görling and N. Rösch, *J. Chem. Phys.* **93**, 5563 (1990).
- [34] U. Fano and J. W. Cooper, *Rev. Mod. Phys.* **40**, 441 (1968).
- [35] P. W. Atkins, *Molecular Quantum Mechanics* (Clarendon, Oxford, 1978), Pt. III.
- [36] H. P. Kelly, *Phys. Rev.* **182**, 84 (1969).
- [37] N. C. Dutta, T. Ishihara, C. Matsubara, and T. P. Das, *Phys. Rev. Lett.* **22**, 8 (1969).
- [38] T. C. Caves and M. Karplus, *J. Chem. Phys.* **50**, 3649 (1969).
- [39] H. P. Kelly and A. Ron, *Phys. Rev. A* **5**, 168 (1972).
- [40] J. D. Jackson, *Classical Electrodynamics*, 2nd ed. (Wiley, New York, 1975).
- [41] P. E. Cade and W. M. Huo, *At. Data Nucl. Data Tables* **15**, 1 (1975).
- [42] M. Rerat, C. Pouchan, M. Tadjeddine, J. P. Flament, H. P. Gervais, and G. Berthier, *Phys. Rev. A* **43**, 5832 (1991).
- [43] V. Kellö, J. Noga, G. H. F. Diercksen, and A. J. Sadlej, *Chem. Phys. Lett.* **152**, 387 (1988).
- [44] N. J. Bridge and A. D. Buckingham, *Proc. R. Soc. London Ser. A* **295**, 334 (1966).